

positive and negative. It can be seen that considering the larger number of metals included, the degree of separation achieved between the two classes of metals is still fairly good. The value of γ lies between +0.5 and -3.4 for superconductors. The only nonsuperconductors for which γ lies in this range are transition elements which are excluded from all the other criteria

except the one by Kikoin and Lasarew which is based on the value of $R\sigma$. A comparison of Fig. 1(a) with Fig. 1(e) shows that the degree of overlapping for γ is, however, smaller than that in $R\sigma$. In conclusion it can be said that the criterion suggested here [Fig. 1(d) and 1(e)] is more successful than any of the others shown in Fig. 1.

PHYSICAL REVIEW

VOLUME 96, NUMBER 4

NOVEMBER 15, 1954

Reversible Susceptibility of Ferromagnetics*

D. M. GRIMES AND D. W. MARTIN

Engineering Research Institute and Department of Electrical Engineering, University of Michigan, Ann Arbor, Michigan

(Received July 6, 1954)

An expression is given relating the magnetization dependence of the reversible susceptibility normal to the field direction to that of the parallel reversible susceptibility. Modification of these susceptibility dependences due to the trapping of domain walls in metastable positions by potential holes is considered. The macroscopic magnetization is expressed in terms of a distribution of potential holes by an argument analogous to that of a "mean free path." The desirability of further examination of this approach is discussed. The reversible susceptibilities of three ferrite specimens were measured and found to compare favorably with the theory.

I. INTRODUCTION

IF one defines a susceptibility by the expression

$$\chi_r = \lim_{\Delta H \rightarrow 0} \frac{\Delta M}{\Delta H}, \quad (1)$$

when ΔH has a sense opposite to that of the change in H which brought the specimen to the point (M, H) , the parallel reversible susceptibility χ_{rp} is defined in the usual manner. When ΔH is perpendicular to the direction of H , the transverse reversible susceptibility χ_{rt} is defined. If ΔH is in the same sense as the last change in total H , the differential susceptibility χ_d is defined. χ_d contains an irreversible component, χ_{rt} and χ_{rp} do not. The initial susceptibility χ_0 is defined as:

$$\chi_0 = \lim_{M \rightarrow 0} \chi_{rp}. \quad (2)$$

The parallel reversible susceptibility in ferromagnetic materials has been the subject of several authors since it was discussed by Gans¹ in 1911. A recent paper by Tebble and Corner² includes a general review. An expression for the transverse reversible susceptibility, given by Grimes, Orr, and Winsnes,³ is developed in this paper. Experimental data are given for both reversible susceptibilities.

To develop expressions for these susceptibilities in terms of the magnetic parameters of a specified system, it is necessary to use different models, depending upon the particular calculation being considered. The models are altered as necessary in the following discussion. The justification for this procedure⁴ is that the susceptibilities depend upon the statistical distribution of potential holes and the relative energy magnitudes involved. It presumably matters little what the specific assumed model is so long as the proper energy relations are maintained.

II. THEORETICAL DEVELOPMENT

A. The Initial Susceptibility

From measurements of the permeability spectrum using particle sizes down to the order of single domains, Rado, Wright, and Emerson⁵ have shown convincingly that the low-frequency initial susceptibility of ferrites is caused primarily by wall movement rather than by rotational processes. It is therefore of interest to note how this susceptibility must depend upon the forces to which the wall is subject.

A plot of the energy of a ferromagnetic body as a function of position x of a given wall would be, over a small region, an irregular curve with many hills and valleys. When no field is present the wall will be found at a minimum position x_1 . If the energy is assumed to be a continuous function of x , then near x_1 ,

$$V(x) = V(x_1) + (1/2\rho_r)(x - x_1)^2 + \dots,$$

* Work supported by the Signal Corps Engineering Laboratories, Fort Monmouth, New Jersey.

¹ R. Gans, *Z. Physik*, **12**, 1053 (1911).

² R. S. Tebble and W. D. Corner, *Proc. Phys. Soc. (London)* **63**, 1005 (1950).

³ Grimes, Orr, and Winsnes, *Phys. Rev.* **91**, 435 (1953).

⁴ W. F. Brown, Jr., *Phys. Rev.* **52**, 325 (1937); *Phys. Rev.* **53**, 482 (1938); *Phys. Rev.* **54**, 279 (1938). These will be referred to as Parts I, II, and III, respectively.

⁵ Rado, Wright, and Emerson, *Phys. Rev.* **80**, 273 (1950).

where ρ_r is the radius of curvature of $V(x)$ at $x=x_1$. When a reversible field dH is applied, the potential of the wall becomes

$$V^*(x) = V(x) - \gamma M_s x dH,$$

for a wall of unit area. γ is a constant depending upon the type of wall. The wall must move to the minimum of $V^*(x)$, so

$$\begin{aligned} dM_r &= \gamma M_s (x - x_1) = \rho_r \gamma^2 M_s^2 dH, \\ \chi_r &\equiv dM_r / dH = \rho_r \gamma^2 M_s^2. \end{aligned} \quad (3)$$

Since this expression applies to a wall of unit area, the problem of explaining the initial reversible susceptibility becomes that of determining the distribution of the wall area per unit volume located at minima of all possible radii ρ_r , and hence also the distribution of such minima.

B. Reversible Susceptibilities

Gans¹ first suggested the parametric equations,

$$M/M_s = f(\eta), \quad \chi_{rp}/\chi_0 = 3f'(\eta), \quad (4)$$

where η was an adjustable parameter and $f(\eta) = L(\eta)$, the Langevin function:

$$L(\eta) = [\coth\eta - (1/\eta)].$$

The prime indicates $d/d\eta$.

These equations were found to fit quite well the data for iron and nickel. They were first derived by Brown⁴ in 1938 by assuming ferromagnetic material to consist of N domains per unit volume all of fixed and equal volume. These domains were considered to be subjected to random but fixed forces in such a manner that the ordinary techniques of statistical mechanics could be applied.

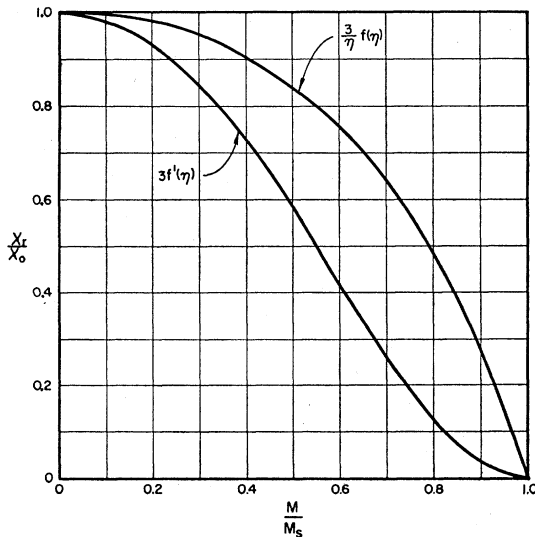


FIG. 1. The parallel and transverse reversible susceptibilities versus magnetization for $f(\eta) = \coth\eta - 1/\eta$.

If the parallel reversible susceptibility is given by Eq. (4), where $f(\eta)$ is a continuous function of η , χ_{rt}/χ_0 can be developed⁶ by assuming that the change in magnetization dM accompanying a change dH_r is such as to keep the total magnetization always parallel to the total field. Then

$$\chi_{rt} \equiv dM/dH_{rt} = M/H_r,$$

where H_r is defined by

$$H_r = \int_0^M \frac{dM}{\chi_{rp}}$$

and is proportional to η . ($\eta = AM_s H_r$.) Therefore,

$$\frac{1}{\chi_{rp}} \equiv \frac{dH_r}{dM} = \frac{d}{dM} \left(\frac{M}{\chi_{rt}} \right).$$

Upon substituting for M and χ_{rp} from Eq. (4) and integrating,

$$\chi_{rt}/\chi_0 = 3f(\eta)/\eta, \quad (5)$$

since $\chi_{rt} = \chi_{rp} = \chi_0$, when $M = 0$.

Brown obtains Eq. (4), from which Eq. (5) follows, for spherical and cubic symmetries. The form of $f(\eta)$ varies with the exact anisotropy type. He found $f(\eta) = \coth\eta - 1/\eta$ for isotropic material, and more complicated expressions for $[111]$ and $[100]$ anisotropies. These three expressions, when expanded for small values of η , are identical up to the seventh order. For the specialized anisotropy types the magnetization vectors are assumed to lie only in the specific easy directions of magnetization. Experimental data should approximate this case only for rather small applied fields, for at higher fields domains will begin to leave these directions to become more nearly aligned with the field. The resulting behavior approaches that of the isotropic case so the isotropic equations should be a good approximation throughout. χ_{rp}/χ_0 and χ_{rt}/χ_0 are plotted vs M/M_s in Fig. 1; the data are given in Table I, column (a).

Brown⁷ later derived Eq. (4) by using a model allowing wall movement and a variation in domain size.

C. Extension of Reversible Theory

For a perfect single crystal with zero demagnetizing factor the application of a small field parallel to an easy direction of magnetization should result in an infinite susceptibility. That it is not infinite in polycrystalline material can be considered to be a result of two different types of forces acting to retard wall movements: reversible and irreversible.

The reversible forces can be considered to arise from intragranular potential minima and from intergranular demagnetizing factors. In the discussion of Sec. A the forces were described in terms of an energy function that was a continuous function of a spatial coordinate. The exact nature of this force distribution cannot be known.

⁶ W. F. Brown, Jr. (private communication).

⁷ W. F. Brown, Jr., Phys. Rev. **55**, 568 (1939).

It would be desirable to be able to predict the qualities of the material which do not depend upon the precise distribution.

That Brown's⁸ W of Part I is very stable with respect to different distributions can be seen by observing that in the neighborhood of the extremum value given by $\partial \ln W / \partial N_\gamma = 0$ higher derivatives of $\ln W$ with respect to N_γ form a polynomial in negative powers of N_γ . An illustration of the stability of this equation would be an application of the equations for isotropic material to [111] or [100] oriented material. The equality to high values of η can be directly attributed to the slowly varying character of W .

We therefore consider the distribution of magnetic moments in a ferromagnetic material when only random reversible forces are applied to be described by Brown's⁴ Eq. (9) of Part I without further definition of the specific "randomness" involved. The resulting magnetic disorder could be considered analogous to a magnetic entropy and should be considered when dealing with magnetic energy problems.

We now wish to discuss susceptibility using statistical arguments to describe the irreversible trapping of domain walls in metastable positions by potential holes. Each hole is to be characterized by a single number, loosely called its "depth" f . A wall encountering such a hole will be trapped if the total net force of the field plus reversible forces on the wall is less than f , but will break free irreversibly if this force exceeds f . Actually these potential minima must surely, for finite wall areas, have a finite radius of curvature. However, for purposes of this discussion we consider them to be infinitely sharp "snags," i.e., a wall is held rigidly when trapped by a potential hole. A wall thus held would contribute nothing to the susceptibility. The true behavior of a ferromagnet must lie somewhere between this model and the model assuming only reversible behavior.

We define n_j to be the fraction of the total number of atoms whose permanent dipole moments are oriented in the direction of the unit vector $\bar{\gamma}_j$. (This is not the same definition Brown uses for n_σ .)

If no potential holes are present when a field \mathbf{H} is applied, according to the reversible equations:

$$n_j = \exp[AM_s(\mathbf{H} \cdot \bar{\gamma}_j)] / \sum_i \exp[AM_s(\mathbf{H} \cdot \bar{\gamma}_i)]. \quad (6)$$

In terms of wall positions, this must also be equal to

$$n_j = \frac{1}{\sum_i \bar{\gamma}_i^2} + \sum_i \sum_\sigma a_{ij}^\sigma x^\sigma, \quad (7)$$

where a_{ij}^σ is the area of a particular wall separating domains oriented in the directions $\bar{\gamma}_i$ and $\bar{\gamma}_j$, respectively, x is the spatial coordinate of the wall relative to a position at which the total net magnetization is zero and Brown's⁴ Eq. (9) Part I is an extremum, and \sum_σ is a sum over all walls of class ij in unit volume.

⁸ See reference 4, part I, p. 326.

TABLE I. Parallel and transverse reversible susceptibilities *versus* magnetization for (a) isotropic material, (b) all atoms either parallel or antiparallel with the applied field, and (c) no atoms making angles greater than $\pi/2$ with respect to the applied field.

M/M_s	χ_{rp}/χ_0			χ_{rt}/χ_0		
	(a)	(b)	(c)	(a)	(b)	(c)
0.0	1.000	1.000	...	1.000	1.000	...
0.2	0.929	0.960	...	0.967	0.983	...
0.4	0.724	0.838	...	0.900	0.946	...
0.5	0.581	0.745	1.000	0.837	0.908	∞
0.6	0.421	0.640	0.923	0.750	0.826	5.67
0.7	0.259	0.526	0.728	0.637	0.804	3.24
0.8	0.119	0.373	0.410	0.480	0.725	1.98
0.9	0.030	0.182	0.012	0.270	0.614	1.08
1.0	0	0	0	0	0	0

If there were no snags, x would be a function, for a given wall, only of the pressure which the applied field exerts, given by

$$p^{ij} = M_s[\mathbf{H} \cdot (\bar{\gamma}_i - \bar{\gamma}_j)].$$

The wall would find an equilibrium position for which the reversible forces just balanced this pressure.

When snags are present walls will become trapped in them, and x will no longer be a simple function of pressure. We can express the average x for a large number of walls in terms of the size distribution of these snags by arguments of the nature of a "mean free path" discussion.

Let the number of snags per unit volume whose depth lies between f and $f+df$ be given by $\xi(f)df$. Let there be an initial state in which there is a field \mathbf{H}_0 present, and all the walls occupy positions x_0 determined only by this field and the reversible forces, i.e., no walls are snagged in metastable positions. When the field is changed to \mathbf{H}_1 , there will be a net force on each wall which will diminish again to zero when the wall reaches a new equilibrium position x_1 . As a wall of area a moves over an interval dx , it sweeps over a volume adx . And if this volume contains a snag "deeper" than the net force of the field plus reversible forces at that place, then the wall will be caught and held there.

Of all the walls in unit volume, let us select for attention the group consisting of all walls of class ij with area between a_{ij}^σ and $a_{ij}^\sigma + da_{ij}^\sigma$. By choosing the coordinates so that x_0 is zero for each wall, then in first approximation the final "reversible" position x_1 of every wall of this select group is equal to the average value \bar{x}_1 , and the net force $f(x)$ of field plus reversible force at each value of x for every wall is equal to some $\bar{f}(x)$ averaged over all the walls.

Let N_0^σ be the number of walls in this group, and $N^\sigma(x)$ the number not yet caught after moving a distance x from x_0 . Then clearly

$$dN^\sigma(x) = -N^\sigma(x) a_{ij}^\sigma dx \int_{\bar{f}(x)}^\infty \xi(f) df,$$

$$N^\sigma(x) = N_0^\sigma \exp \left[-a_{ij}^\sigma \int_0^x dx' \int_{\bar{f}(x')}^\infty \xi(f) df \right].$$

The fraction of the original group of walls that becomes snagged in the interval x to $x+dx$ is then

$$\Psi^\sigma(x)dx = |dN^\sigma(x)|/N_0^\sigma = \left(\exp \left[-a_{ij}^\sigma \int_0^x dx' \right. \right. \\ \left. \left. \times \int_{\bar{f}(x')}^\infty \xi(f)df \right] a_{ij}^\sigma \int_{\bar{f}(x)}^\infty \xi(f)df \right) dx,$$

and the average position at which the walls of the group considered become snagged and stop is

$$\bar{x}^\sigma = \int_0^{\bar{x}_1} x \Psi^\sigma(x) dx. \quad (8)$$

Apart from the idealization of the potential holes as sharp snags, the most tenuous point of the above discussion is the use of the average net force function $\bar{f}(x)$. The reversible forces actually may vary greatly from wall to wall. In keeping with the original idealization, all local irregularities in the $f(x)$ of any individual wall may be lumped in with the snags, leaving only a smooth curve which decreases from a maximum at $x=0$ to zero at x_1 . There still remains the possibility of large differences in $f(0)$ from wall to wall. But this is no difficulty in principle, for one could merely further subdivide the groups of walls into subgroups according to the value of $f(0)$, assume a distribution in numbers of walls in the subgroups, and sum the results over the subgroups. The same comments apply to the use of the average \bar{x}_1 in the calculation.

The point is that if the sole object of the formula were the explicit calculation of magnetization curves, one could undoubtedly build enough assumptions and parameters into it by refinements of this type to fit any amount of experimental data. It is surely doubtful if this would be sensible in view of the extreme idealization of the model. It remains of some interest to see if some rough quantitative agreement could not be obtained with the expression in its simplest form, using reasonable assumptions for $\xi(f)$. Such a check is desirable to see if this type of analysis does have any real validity, but this has not yet been done.

However, one important conclusion follows from the form of Eq. (8) independent of these details. To the same approximation as that contained in Eq. (8), the quantity x^σ to be used in Eq. (7) for the strictly reversible case is exactly the average "final reversible" coordinate \bar{x}_1 that appears as the upper limit in Eq. (8). Now \bar{x}_1 must have a certain (perhaps quite complicated) dependence on the relative directions of $\bar{\gamma}_i$, $\bar{\gamma}_j$, and the applied field \mathbf{H} that is consistent with the existence of Eq. (6) for the reversible case. Without any detailed analysis it is clear that \bar{x}^σ has additional dependence on these directions arising in the expression for $\Psi^\sigma(x)$. So the distribution in numbers of atoms oriented in the

various possible directions, in the presence of "snags" and metastable wall positions, is different from that implied by an expression of the form of Eq. (6). This amounts to saying that it is not possible to define any simple vector "effective field" \mathbf{H}' that allows a description of the system in terms of Eq. (6). Brown⁹ has shown that only if such a vector field exists do the parametric Eqs. (4) hold. Therefore we do not expect them to be strictly true.

The understanding that the affect of the irreversible forces on Eqs. (4) and (5) arises through a redistribution of populations in the various possible directions suggests a simplified approach. One can say that effectively the material has certain peculiar unsymmetrical anisotropy properties that will also lead to a redistribution of atomic moments. It is shown below that certain qualitative features can be correctly predicted very simply in this way for a few special circumstances for which the direction of this redistribution is apparent.

D. Modifications of the Reversible Model

Contribution of Metastable Volume

The reversible susceptibility of a ferromagnetic material is decreased from the value predicted by the reversible equations by the presence of intragrain potential holes. In general, the greater the depth of a minimum the smaller is its radius of curvature, and therefore the less a wall occupying it will contribute to the susceptibility. The decrease should become larger as the peak M reached during a cycle increases, causing walls to cross potential barriers capable of retaining them in deep metastable states. In general, it would not be the same holes that would decrease the two different susceptibilities.

High M/M_s , Decreasing $|\mathbf{M}|$

When $|\mathbf{M}|/M_s=1$, all the material is necessarily aligned with the applied field. As $|\mathbf{M}|$ is decreased from M_s the metastable volume will be predominantly oriented in the direction of M_s . The remainder we take to be oriented in accordance with the reversible equations. Since the number of atoms with their magnetic moments parallel with the biasing field is increased by the action of the potential holes, at a specified value of M there must also be more atoms aligned antiparallel than would otherwise be the case. Since the number of atoms is fixed this must also mean that the number of atoms oriented in all other directions is diminished.

To find qualitatively how this affects the susceptibilities, consider an extreme case where all magnetic moments are oriented either parallel or antiparallel with the field. Brown's⁴ Eq. (3) of II then becomes

$$M/M_s = \tanh \eta,$$

where, as usual, $\eta = AM_s H r$.

⁹ See reference 7, p. 574.

This leads to:¹⁰

$$\chi_{rp}/\chi_0 = \operatorname{sech}^2 \eta; \quad \chi_{rt}/\chi_0 = \tanh \eta / \eta. \quad (9)$$

Values of χ_{rp}/χ_0 and χ_{rt}/χ_0 vs M/M_s are given in Table I. Both curves are higher than the corresponding curve for isotropic material, but are of the same order and of the same general form.

High M/M_s , Increasing $|M|$

In the randomly oriented state, none of the volume is in a metastable condition, but after the application of an external field a finite fraction of the material will be. Those domain walls which are located between atoms with moments parallel and antiparallel to the field will move the farthest when a field is applied. Therefore the fraction of the atoms which find themselves in metastable positions should be greatest for those atoms oriented antiparallel to the field, and zero for those oriented parallel. As the magnetization increases, however, the amount of material available to be held in these metastable states is least for antiparallel and greatest for parallel alignment. Therefore at all values of magnetization greater than a certain minimum, the number of atoms whose magnetic moments are held in metastable positions must go through a maximum at some angle between 0 and π , and so for a given η the normal component of magnetization is increased. It then follows that for a specified M the total magnetic moment both parallel and antiparallel with the field is decreased, while the difference remains constant.

In the limiting case, the number of atoms antiparallel decreases to zero, i.e., no atoms possess magnetic moments making angles greater than $\pi/2$ with the applied field. For this case the magnetization would be given by:

$$\frac{M}{M_s} = \left(\frac{e^\eta}{e^\eta - 1} - \frac{1}{\eta} \right).$$

For small fields,

$$M/M_s = \frac{1}{2} + \eta/12 + \dots$$

The resulting susceptibilities are given by:¹¹

$$\begin{aligned} \frac{\chi_{rp}}{\chi_0} &= 12 \left\{ \frac{1}{\eta^2} - \frac{e^\eta}{(e^\eta - 1)^2} \right\}, \\ \frac{\chi_{rt}}{\chi_0} &= \frac{12}{\eta} \left\{ \frac{e^\eta}{e^\eta - 1} - \frac{1}{\eta} \right\}. \end{aligned} \quad (10)$$

χ_0 is the value of the parallel reversible susceptibility when $\eta=0$. From this model, $\chi_{rt} \neq \chi_{rp}$, when $\eta=0$.

¹⁰ The integration constant in χ_{rt}/χ_0 must be zero for symmetry to exist about $\eta=0$.

¹¹ To evaluate the integration constant note that χ_{rt} must become infinite at some value of M/M_s . It will be positive above that value and negative below. The only point where such a discontinuity can exist is for $\eta=0$. Thus the integration constant must be zero.

Values of M/M_s , χ_{rp}/χ_0 , and χ_{rt}/χ_0 are given in Table I.

Obviously χ_{rt}/χ_0 is much greater for this model than for the isotropic model.

III. EXPERIMENTAL METHOD

Experimental data were taken to (a) check the validity of the equations describing χ_{rt} vs M , and (b) to see if deviations from the predicted values of χ_{rp} and χ_{rt} vs M using $f(\eta) = L(\eta)$ can be explained in terms of the discussion of the previous section.

The gross magnetization of the samples is excited by a battery-powered dc field, and is measured by the change of flux through windings on the sample when this "bias field" is abruptly changed. This measurement is made with a General Electric fluxmeter. Susceptibility was measured by observing, with a vacuum tube voltmeter the voltage developed across a winding on the sample when a 5 kc/sec current of small known amplitude was driven in the same winding. The flux is assumed to be in phase with the current, so that the induced voltage lags the ohmic voltage by 90° .

A toroidal specimen shape was chosen so that the conflicting requirements for both the parallel and transverse susceptibility measurements could be met by the same sample as far as possible. Closed flux paths around the ring eliminate demagnetizing effects for fields in this direction, while the lateral extent of the specimen is confined so that homogeneous transverse fields may be more readily applied. Susceptibility is measured in both cases around the ring using a toroidal winding. For the parallel case, the bias field is applied by a second toroidal winding, while for the transverse case it is applied along the toroidal axis by an external electromagnet.

Magnetization Measurements

In the parallel case, the applied field varies with position but its average value can be accurately calculated, except for small leakage effects, from the current. The sensing winding detects the total change in flux which is proportional to the average induction. The difference is 4π times the average magnetization. There is considerable difficulty in the determination of the saturation magnetization. The plot of M is still increasing at fields over 200 oersteds, at which value leakage is becoming important and ohmic heat excessive. We obtained the plot this far, and then fitted a Langevin function to the last two points to obtain an estimate of M_s that is believed good to 10 percent. Error in this value affects the normalization of the abscissas of the χ_{rp} vs M curves.

In the transverse case the applied field is not known from the bias current, here applied to the electromagnet, because of reluctance and hysteresis of the magnet. It is taken equal to the flux density through the hole in the center of the toroid. This value is measured relative to a

reproducible starting point by observing as the magnet current is cycled, the flux changes in a search coil which embraces the hole. The total flux through the core volume is measured using a girdle winding placed snugly about the inner and outer peripheries of the toroid.

The difference of these two readings we call the apparent magnetization M_a . By an elementary calculation $M_a = (1 - N/4\pi)M$, where $N/4\pi$ is the demagnetizing factor. If the geometry is such that the magnetization is homogeneous, then $N/4\pi$ will be constant independent of M , and the ratio of M_a to the apparent saturation value M_{sa} will be strictly equal to the true ratio M/M_s . We thus obtain the properly normalized abscissa without having to determine the demagnetizing factor or the true M_s . To this end, the magnet was built with accurately parallel plane pole faces and a continuously adjustable gap that can be fitted snugly against the windings of the sample. The magnet readily provides very high fields that yield a well defined value of the apparent saturation M_{sa} .

Susceptibility Measurements

In the transverse case the bias magnetization is assumed to be homogeneous, so that the susceptibility is constant throughout the sample. In the parallel case, however, the bias field varies inversely as the radius from the axis of the toroid, so the magnetization and the susceptibility also vary. The observed average of the susceptibility is $4\pi\bar{\chi} = (\bar{\mu}_\Delta - 1)$, where $\bar{\mu}_\Delta$ is proportional to the ratio of an induced voltage to a current, and hence

$$\bar{\mu}_\Delta = \frac{\overline{\Delta B}}{\overline{\Delta H}} = \frac{\int \mu \Delta H dr}{\int \Delta H dr}.$$

Since ΔH is applied by a toroidal winding, it varies as $1/r$, so

$$\bar{\mu}_\Delta = \frac{\int \frac{\mu}{r} dr}{\int \frac{1}{r} dr}.$$

Thus,

$$\bar{\chi} = \frac{1}{\ln(r_2/r_1)} \int_{r_1}^{r_2} \frac{\chi(r)}{r} dr, \quad (11)$$

where r_1 and r_2 are the inner and outer radii of the toroid, respectively.

It is necessary to calculate this average from the theoretical curves in order to compare with experiment. Because the theory gives only the dependence of χ on M , one must know how M depends on H , which varies as $1/r$, to evaluate the integral. We have made two different simplified assumptions for the $M-H$ loop which represent opposite extremes of observed behaviors. We calculated the integral (11) numerically for each, using the theoretical $\chi-M$ relation. The resulting $\bar{\chi}$ vs \bar{M} curves are found to be much alike, and each differs from the uncorrected curve in essentially the same way. Since the result is so insensitive to the details of this assumption, and in view of the uncertainties in our data, it is felt that the labor of preparing a separate curve especially fitted to the experimental $M-H$ loop of each sample would be excessive, particularly since this latter curve is itself only a relation of averages. Therefore a compromise curve displaying the general features of the two special cases has been used for comparison with experiment in all cases.

This compromise curve appears as the theoretical transverse curve in Fig. 2. The two cases for which it represents the average are:

- (1) The $M-H$ loop is a parallelogram:

$$M = \beta M_s (H/H_c \pm 1); \quad -M_s < M < M_s.$$

- (2) The $M-H$ loop is two displaced Langevin functions:

$$M = M_s L[K(H/H_c \pm 1)],$$

where H_c is the coercive force. The free parameters β and K are given the values 0.2 and 0.615, respectively,

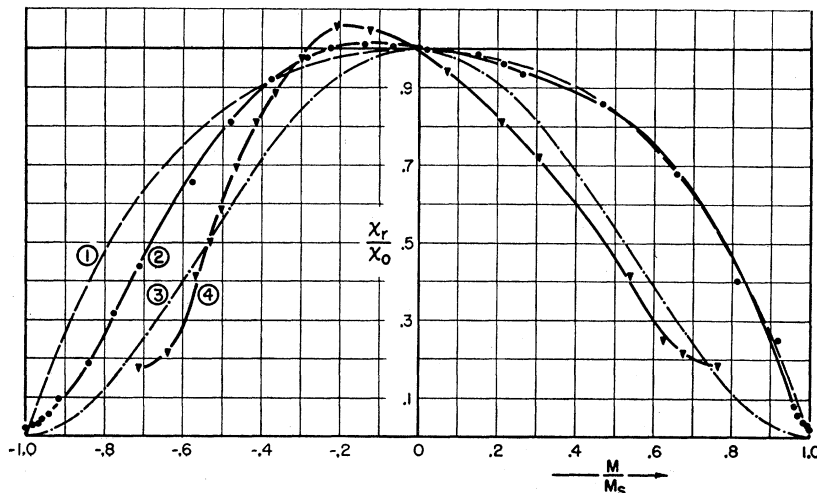


FIG. 2. Parallel and transverse reversible susceptibility vs magnetization. The dashed curves are the theoretical curves, with $f(\eta) = \coth \eta - 1/\eta$. The solid curves represent experimental measurements. (Core E-3, 25°C.) Curves ① and ② are for transverse, ③ and ④ for parallel susceptibility. Curve ③ incorporates the corrections due to geometric averaging (Sec. III).

to fit these assumptions to the criterion that remanent magnetization $M_R = 0.2M_s$. The result is further specialized in that the ratio r_1/r_2 is taken as 0.5.

IV. EXPERIMENTAL RESULTS AND COMPARISON WITH THEORY

Data were taken mainly on three cores purchased from the General Ceramics and Steatite Corporation, Keasby, New Jersey, representing their types *E*, *G*, and *I* ferrites. Most measurements were made at room temperature, but some were made up to 100°C. The interesting features of the data were virtually identical in all cases.

For two of the samples the apparent saturation magnetization was about 20 percent less than the extrapolated parallel value, indicating an effective demagnetizing factor of about 0.2 for the transverse geometry. The third sample was about 50 percent thicker than the others, and gave equal values of M_s for both cases. Evidently the increased thickness sharply reduces the demagnetizing factor. As expected, this produces no noticeable effect on the normalized χ_{rp} vs M curve.

In Fig. 2 are shown the parallel and transverse curves for a typical case compared with the corresponding theoretical curves. In Fig. 4 the same curves are shown separately plotted on a folded abscissa for comparison of the ascending and descending branches of each, together with a similar plot of χ_{rp} vs the applied field. In Fig. 3 are shown the parallel curves from three different minor loops, in which the peak value of M reached in the cycle is varied.

The curves of Fig. 2 are normalized to the value of χ at $M=0$ on the loop in question, for convenience in comparison with the theoretical curves. The actual χ_0 obtained when the sample is fully demagnetized is always larger than this, and in fact always exceeds the peak values of all these curves as expected. Note that the experimental curves lie generally below the theoretical curves, although with this normalization they lie higher in the region of the maximum. This is in keeping with the previous remark that potential irregularities always act to decrease the susceptibility.

In Fig. 2, the maximum in both cases lies to the left of zero, on the side of decreasing $|M|$. We can understand this in terms of the trapping of walls by snags. The contribution to the reversible susceptibility of any wall caught by a snag is always diminished. Idealizing this, imagine that on a given loop a certain fraction D of the volume of the sample be held in metastable condition by snags, and contributes nothing to χ_r . Then the total susceptibility of the sample will be maximum when the magnetization of the remaining free volume $(1-D)$ is zero. The metastable volume D will, however, still contribute a net magnetization in the direction of the last previous maximum of M .

The shifting of the susceptibility peak with M_{\max} of

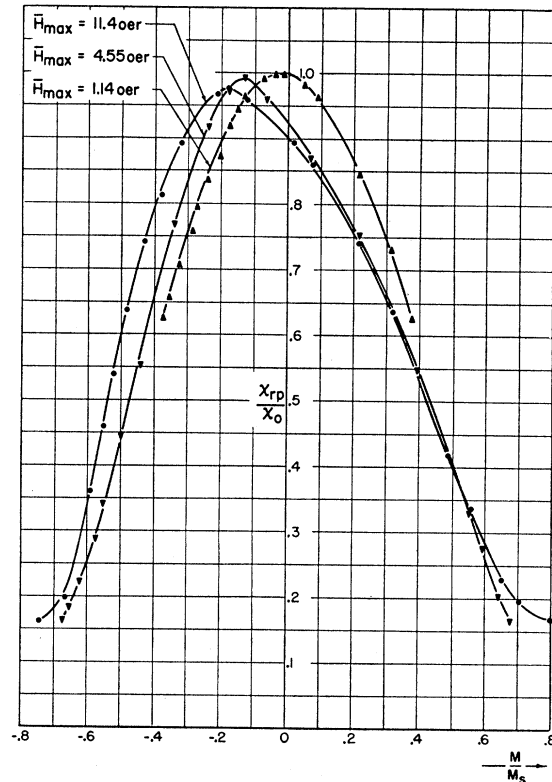


Fig. 3. Variation with peak $|M|$ of the value of M/M_s at which maximum χ_{rp} occurs. (Core E-3, 25°C.)

Fig. 3 can be understood in the same way. As the peak M of the cycle is increased, the fraction D which is forced over into deep metastable positions would evidently also increase. This will obviously shift the susceptibility peak further to the left and diminish its height, as observed. The given curves apply to the parallel case. The same behavior is expected for the transverse case, but minor loop curves could not be accurately obtained with our procedures.

The location of the susceptibility peak on the decreasing $|M|$ branch causes this whole branch to lie generally higher than the ascending $|M|$ branch. In Fig. 4 it is seen that this is true everywhere for the parallel case, and also at low values of magnetization in the transverse case. However, the discussion of Sec. II indicates that for the transverse case, larger values of χ are to be expected on the ascending branch than on the descending branch. In Fig. 4 one sees that the curves do cross over at high M/M_s . The location of this crossover would be expected to shift to lower M/M_s as M_{\max} was decreased.

According to Tebble and Corner,² the peak in susceptibility occurs at values of M less than remanence. Thus, a plot of χ vs the applied field H has its maximum where H is increasing from zero, but is less than the coercive force. Our data for the parallel case, illustrated by the last graph of Fig. 4, agree with this. Note in the

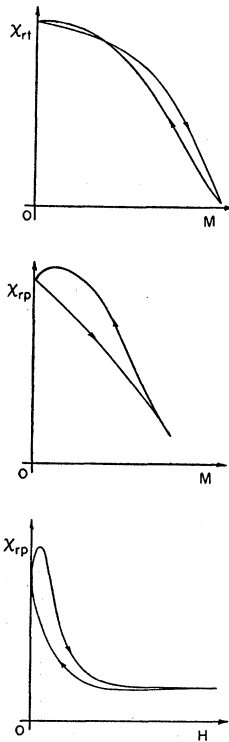


FIG. 4. Comparison of the hysteresis loops for χ_{rp} vs M and H , and for χ_{rt} vs M .

figure that although the χ vs M and χ vs H loops look much alike, the directions of travel around them are opposite.

In the transverse case we know the net applied field only very uncertainly, as a small difference of very large terms. Therefore we do not have any good measure of transverse remanence. For two of the samples the transverse susceptibility peak occurs at a value of M/M_s less than the corresponding parallel remanence, but for the third sample the peak is broad and occurs at an

M/M_s equal to or perhaps a little greater than the parallel remanence.

The accuracy of our susceptibility measurements was limited by the noise reading on our instrument for measuring the voltage drop across the toroid, (Hewlett Packard 400C VTVM) and our ability to read the meter. The normalized data are considered accurate within ± 5 percent, the absolute values accurate within ± 8 percent.

With the exception of the parallel field measurement of M_s , our magnetization data are limited in accuracy by fluxmeter drift and errors in meter reading. These are considered to be well within ± 5 percent.

V. SUMMARY AND CONCLUSIONS

As far as the authors are aware, the statistical approach to the dependence of macroscopic magnetization on magnetic history that is presented herein has not been suggested previously. While the result quoted is still too general to permit any direct evaluation against experiment, it is felt that it might form a worth-while basis for more detailed analysis. Of more immediate interest is the fact that the general arguments provide basis and motivation for the simple special models devised to predict various general features of the behavior of a ferromagnet. The quoted experimental results indicate that, idealized though they are, these models do provide a qualitative basis for understanding.

While the experimental results presented were all obtained from ferrites, the general theory of course applies to all ferromagnets. However, the more special parts of the discussion would not apply to crystals of lower symmetry without modification.

The authors wish to acknowledge the aid of Professor E. Katz during early stages of the work, Professor H. W. Welch, Jr., for his aid and encouragement, and to Mr. John Newton and Mr. Ralph Olson for their assistance in gathering data.